Dispersion Characteristics of Organoclay in Nanocomposites Based on End-Functionalized Homopolymer and Block Copolymer

Weibin Zha, Soobum Choi, Kyung Min Lee, and Chang Dae Han*

Department of Polymer Engineering, The University of Akron, Akron, Ohio 44325

Received April 15, 2005; Revised Manuscript Received July 19, 2005

ABSTRACT: The dispersion characteristics of organoclay in nanocomposites based on end-functionalized polystyrene (PS) and end-functionalized polystyrene-*block*-polyisoprene (SI diblock) copolymer were investigated using X-ray diffraction (XRD), transmission electron microscopy (TEM), and oscillatory shear rheometry. For the study, a low-molecular-weight polystyrene (PSLMW), having molecular weight (M) lower than the viscosity critical molecular weight (M_c), and a high-molecular-weight polystyrene (PSHMW), having $M > M_c$, were synthesized via anionic polymerization. Each polystyrene (PS) was terminated by carboxylic acid (−COOH) group via carbonation, yielding PSLMW-t-COOH or PSHMW-t-COOH, which were then neutralized, yielding PSLMW-t-COONa or PSHMW-t-COONa. Further, two SI diblock copolymers were synthesized via anionic polymerization. In so doing, the PS block or PI block were end-functionalized via carbonation to yield IS-t-COOH or SI-t-COOH, which were then neutralized to obtain IS-t-COONa or SI-t-COONa. Each of the end-functionalized polymers was mixed in a cosolvent of tetrahydrofuran and water with an organoclay (Southern Clay Products) to prepare nanocomposites. It has been found via XRD and TEM that the polymers terminated by sodium carboxylate (−COONa) group are much more effective in dispersing organoclay aggregates than the polymers terminated by −COOH group. The ionic interaction between the negatively charged carboxylic ion ($-COO^-$) at the polymer chain end and positively charged N^+ ion in the surfactant residing at the surface of organoclay is believed to be the driving force that has enhanced the dispersion of organoclay aggregates, giving rise to a very high degree of dispersion. The rheological measurements at elevated temperatures, via oscillatory rheometry, indicate that the storage modulus of the nanocomposites based on end-functionalized polymers is considerably higher than that of neat end-functionalized polymers. This observation is attributed to ionic interactions between the negatively charged anion at polymer chain end and the positively charged ion in the surfactant residing at the surface of organoclay.

1. Introduction

During the past decade, very extensive research efforts on the preparation of organoclay nanocomposites have been reported in the literature from both the academic and industrial communities. The basic premise for the preparation of organoclay nanocomposites is that well-dispersed organoclay would significantly improve the mechanical properties and certain thermal/physical characteristics (e.g., heat distortion temperature, gas barrier properties) of the nanocomposite. Such a premise is based on the notion that very well-dispersed organoclay (a very high degree of exfoliation) will significantly increase the surface areas of the organoclay. This then suggests that one must strive to achieve a very high degree of exfoliation when organoclay nanocomposites are prepared. In the preparation of organoclay nanocomposites, exfoliation is preferred to intercalation.

Organoclay nanocomposites have been prepared by two methods: (i) by in situ polymerization, and (ii) by melt blending or solution blending. In conducting in situ polymerization, monomers with functional groups are polymerized in the presence of chemically modified layered silicates, such that the exfoliated layered silicates can be associated with the polymer matrix. This method was first introduced by Toyota scientists,[1] and later, other research groups[2−4] prepared organoclay nanocomposites using the same method. This approach has an advantage over melt blending or solution blending in that it can give rise to a very high degree of exfoliation of layered silicate aggregates in the nanocomposites. This is because the viscosity of monomers is so low that they can easily approach the layered silicate aggregates, while vigorously stirring, to separate the top and bottom layers as promoted by the application of shear stress. However, in situ polymerization of monomers in the presence of chemically modified layered silicates is not always possible (e.g., in anionic polymerization), and thus, under such circumstances, melt blending or solution blending must be employed to prepare organoclay nanocomposites.

When a thermoplastic polymer is mixed with an organoclay, intercalation is observed when a polymer matrix and layered silicates do not have sufficient attractive interactions, while exfoliation is observed when a polymer matrix and layered silicates have strong attractive interactions. It is well established that natural clay (montmorillonite) is an aggregate of layered silicates,[5,6] exfoliation of which is very difficult to achieve by strictly mechanical forces during compounding, for instance, in an extruder. Thus, efforts have been spent on chemical modifications of the surface of layered silicates using a surfactant(s), the role of which is to provide *attractive interactions*, during mixing, with a thermoplastic polymer. It is then very clear that there should be a chemical affinity between a surfactant residing at the surface of layered silicates and a thermoplastic polymer. This concept is nothing different from the concept that has long been used in the preparation of miscible polymer blends. This means that, in the preparation of exfoliated organoclay nanocomposites, one must choose a right combination of the

* Author to whom correspondence should be addressed. E-mail: cdhan@uakron.edu.

10.1021/ma050803c CCC: $30.25
Published on Web 09/02/2005

chemical structure of a surfactant residing at the surface of layered silicates and the chemical structure of a thermoplastic polymer.

There are several hundreds of papers[7] that have reported on the preparation of organoclay nanocomposites having varying degrees of dispersion. Review articles[8−11] and our recent papers[12,13] have cited some selected papers. The majority of the papers have reported on intercalated nanocomposites, owing to the lack of sufficient attractive interactions between the organoclay and the polymer matrix chosen. Attractive interactions between a surfactant residing at the surface of an organoclay and a polymer matrix can occur by different mechanisms, such as hydrogen bonding, ionic interaction, dipole−dipole interaction, the formation of electron donor−acceptor complexes, etc.

In our previous publications, we have shown that hydrogen bonds were formed between a surfactant, which had hydroxyl groups, residing at the surface of organoclay and polycarbonate (PC),[12] poly(ethylene-*co*-vinyl acetate-*co*-vinyl alcohol) (EVAOL),[13] polystyrene-*block*-hydroxylated polyisoprene (SIOH diblock) copolymer,[14] or polyisoprene-*block*-polystyrene-*block*-hydroxylated polybutadiene (ISBOH triblock) copolymer.[15] The formation of hydrogen bonds then yielded a high degree of exfoliation of organoclay. We have also shown[15] that the location of a functionalized block in a triblock copolymer had a profound influence on the effectiveness of dispersing organoclay aggregates. Specifically, we have shown that the hydroxylation of the polybutadiene (PB) endblock in a polyisoprene-*block*-polystyrene-*block*-polybutadiene (ISB triblock) copolymer was very effective, while the hydroxylation of the polyisoprene (PI) midblock in a polystyrene-*block*-polyisoprene-*block*-polystyrene (SIS triblock) copolymer was not, in dispersing organoclay aggregates. The above experimental observations prompted us to investigate the effectiveness of end-functionalization of homopolymer or block copolymer on the dispersion characteristics of organoclay aggregates. However, to date, there have been very few experimental studies[16] reporting on the dispersion characteristics of organoclay aggregates in nanocomposites based on end-functionalized polymer.

Very recently, we prepared organoclay nanocomposites by synthesizing, via anionic polymerization, polystyrenes (PS) and polystyrene-*block*-polyisoprene (SI diblock) copolymers, each terminated by carboxylic acid group (−COOH) or sodium carboxylate group (−COONa). Then we investigated the dispersion characteristics of organoclay aggregates in the nanocomposites based on the end-functionalized PS or end-functionalized SI diblock copolymers using X-ray diffraction (XRD), transmission electron microscopy (TEM), and oscillatory shear rheometry. Our focus was on the investigation of the dispersion characteristics of the organoclay aggregates in the nanocomposites as affected by the molecular weight of end-functionalized PS, the chemical structure of the functional groups at a chain end of PS or SI diblock copolymer, and the chemical structure of a surfactant residing at the surface of an organoclay. In this paper, we present the highlights of our findings.

2. Experimental Section

Synthesis and Characterization of End-Functionalized PS and End-Functionalized SI Diblock Copolymer. Using the standard procedures for anionic polymerization with *sec*-butyllithium as initiator, we synthesized two polystyrenes (PS): a low-molecular-weight polystyrene (PSLMW) with molecular weight (M) lower than the viscosity critical molecular weight (M_c) and a high-molecular-weight polystyrene (PSHMW) with $M > M_c$. After completion of anionic polymerization of PSLMW or PSHMW, each polymer was subjected to carbonation to terminate the chain end with carboxylic acid group (−COOH) by introducing high purity, gaseous carbon dioxide (CO_2), yielding PSLMW-t-COOH or PSHMW-t-COOH. The details of carbonation procedures employed are described in the literature.[17,18] The two end-functionalized PSLMW-t-COOH and PSHMW-t-COOH were synthesized to investigate whether the molecular weight has any effect on the dispersion characteristics of organoclay aggregates in nanocomposites. To investigate the effect of the chemical structure of the functional group at chain end on the dispersion characteristics of organoclay aggregates in nanocomposites, PSLMW-t-COOH and PSHMW-t-COOH, respectively, were dissolved in toluene and then neutralized by adding an excess amount of sodium hydroxide (NaOH)/methanol mixture, while vigorously stirring, yielding PSLMW-t-COONa and PSHWM-t-COONa.

Table 1. Molecular Characteristics of the Polystyrenes and SI Diblock Copolymers Synthesized for End Functionalization

sample code	M_w[a]	M_w/M_n[a]	w_{PS}[b]
PSLMW	2.7×10^4	1.06	
PSHMW	7.0×10^4	1.03	
SI-1	1.7×10^4	1.09	0.45
SI-2	1.9×10^4	1.07	0.47

[a] Determined from GPC. [b] Weight fraction of polystyrene block determined by ^{1}H NMR spectroscopy.

Also, we synthesized, via anionic polymerization using *sec*-butyllithium as initiator, two SI diblock copolymers and then terminated the chain end, via carbonation, with a −COOH group. In one instance, isoprene (I) monomer was first polymerized followed by the polymerization of styrene (S) monomer, and then the PS block was terminated, via carbonation, by a −COOH group, yielding IS-t-COOH. In another instance, styrene monomer was first polymerized, followed by the polymerization of isoprene monomer, and then the polyisoprene (PI) block was terminated by a −COOH group, yielding SI-t-COOH. Subsequently, IS-t-COOH and SI-t-COOH, respectively, were neutralized, yielding IS-t-COONa and SI-t-COONa.

The chemical structures and the compositions of the end-functionalized polystyrenes and end-functionalized SI diblock copolymers were confirmed using ^{1}H nuclear magnetic resonance (NMR) spectroscopy, and the molecular weight and molecular weight distribution were determined, via gel permeation chromatography, against polystyrene standards. Thus the molecular weights determined are relative values. Table 1 gives a summary of sample codes and the molecular characteristics of two polystyrenes and two SI diblock copolymers synthesized in this study. The molecular weights summarized in Table 1 were measured by dissolving polymer samples in tetrahydrofuran (THF) as solvent.

Preparation of Organoclay Nanocomposites. To prepare nanocomposites based on the end-functionalized PS or end-functionalized SI diblock copolymer, we employed natural clay, montmorillonite (Southern Clay Products), and two commercial organoclays (Southern Clay Products): (i) Cloisite 30B, treated with a surfactant (MT2EtOH), having the chemical structure methyl, tallow, bis-2-hydroxyethyl, and quaternary ammonium chloride, and (ii) Cloisite 20A, treated with a surfactant (2M2HT), having the chemical structure methyl, hydrogenated tallow, and quaternary ammonium chloride. The chemical structures of the surfactants, MT2EtOH and 2M2HT, are given below[19] In the chemical structure of MT2EtOH, N^+

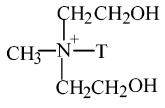

MT2EtOH

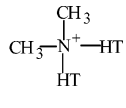

2M2HT

Table 2. Sample Codes of the Nanocomposites Investigated in This Study[a]

sample code	functionality
(a) End-Functionalized PS/Organoclay Nanocomposites	
(PSLMW-t-COOH)/Cloisite 20A	−COOH terminated low-molecular-weight PS
(PSLMW-t-COOH)/Cloisite 30B	−COOH terminated low-molecular-weight PS
(PSLMW-t-COONa)/Cloisite 20A	−COONa terminated low-molecular-weight PS
(PSLMW-t-COONa)/Cloisite 30B	−COONa terminated low-molecular-weight PS
(PSHMW-t-COOH)/Cloisite 20A	−COOH terminated high-molecular-weight PS
(PSHMW-t-COOH)/Cloisite 30B	−COOH terminated high-molecular-weight PS
(PSHMW-t-COONa)/Cloisite 20A	−COONa terminated high-molecular-weight PS
(PSHMW-t-COONa)/Cloisite 30B	−COONa terminated high-molecular-weight PS
(b) End-Functionalized SI Diblock Copolymer/Organoclay Nanocomposites	
(SI-t-COOH)/Cloisite 20A	PI block in SI-1 was terminated by −COOH group
(SI-t-COOH)/Cloisite 30B	PI block in SI-1 was terminated by −COOH group
(SI-t-COONa)/Cloisite 20A	PI block in SI-1 was terminated by −COONa group
(SI-t-COONa)/Cloisite 30B	PI block in SI-1 was terminated by −COONa group
(IS-t-COOH)/Cloisite 20A	PS block in SI-2 was terminated by −COOH group
(IS-t-COOH)/Cloisite 30B	PS block in SI-2 was terminated by −COOH group
(IS-t-COONa)/Cloisite 20A	PS block in SI-2 was terminated by −COONa group
(IS-t-COONa)/Cloisite 30B	PS block in SI-2 was terminated by −COONa group

[a] All nanocomposites have 5 wt % organoclay.

denotes quaternary ammonium chloride, and T denotes tallow consisting of ca. 65% C18, ca. 30% C16, and ca. 5% C14, and in the chemical structure of 2M2HT, N^+ denotes quaternary ammonium chloride, and HT denotes hydrogenated tallow consisting of ca. 65% C18, ca. 30% C16, and ca. 5% C14. It should be mentioned that 100% of Na^+ ions in montmorillonite (MMT) have been exchanged.[19] According to the Technical Properties Bulletin[19] from Southern Clay Products, the amount of surfactant MT2EtOH residing at the surface of Cloisite 30B is 90 mequiv/100 g, and the amount of surfactant 2M2HT residing at the surface of Cloisite 20A is 95 mequiv/100 g. We have been informed by Southern Clay Products that a very small amount of excess surfactant is present at the surface of each organoclay. The two organoclays were used to investigate the effect of the chemical structures of surfactants, MT2EtOH and 2M2HT, on the interactions with the functional groups attached at the chain end of the polymers synthesized in this study and thus on the dispersion characteristics of organoclay in nanocomposites.

We prepared sixteen organoclay nanocomposites by solution blending; namely, a predetermined amount of end-functionalized PS or SI diblock copolymer was dissolved in a cosolvent of tetrahydrofuran (THF) and water (H_2O) (90:10 v:v), and then an organoclay in a cosolvent of THF/H_2O mixture was added slowly, while stirring, into the polymer solution. Before use, each of the organoclays was washed with methanol. The solvent in the mixture was evaporated slowly in a fume hood for 2 days and then dried further in a vacuum oven at temperatures well above the boiling point of the solvent and also at ca. 20 °C above the glass transition temperature (T_g) of the polymer until no weight changes were detected. Table 2 gives a summary of sample codes of the sixteen organoclay nanocomposites prepared. The amount of organoclay used was 5 wt % in all nanocomposites. Because the amount of surfactant MT2EtOH or 2M2HT on the surface of Cloisite 30B or Cloisite 20A is 32 wt %, the net amount of clay was 3.4 wt % in each nanocomposite. For comparison, we also prepared (PSLMW-t-COOH)/MMT and (PSLMW-t-COONa)/MMT nanocomposites, in which the amount of MMT used was 5 wt %.

X-ray Diffraction (XRD). Wide-angle X-ray scattering was conducted at ambient temperature on a Rigaku Rotaflex rotating anode diffractometer with slit collimation. The X-ray generator was operated at 40 kV and 150 mA, and the X-ray beam was monochromatized to Cu K_α with a graphite crystal. The range of 2θ scanning of X-ray intensity employed was 1.5−10 degrees. X-ray diffraction (XRD) patterns were obtained to determine the mean interlayer spacing of the (001) plane (d_{001}) for the organoclay (Cloisite 20A or Cloisite 30B) and its nanocomposites with an end-functionalized PS or end-functionalized SI diblock copolymer.

Transmission Electron Microscopy (TEM). TEM images of specimens were taken at room temperature. The ultrathin sectioning (50−70 nm) was performed by ultramicrotomy at room temperature for the nanocomposites based on end-functionalized PS, and at − 70 °C for the nanocomposites based on end-functionalized SI diblock copolymer using a Reichert Ultracut E low-temperature sectioning system. A transmission electron microscope (JEM1200EX 11, JEOL) operated at 120 kV was used to obtain images of nanocomposite specimens.

Oscillatory Shear Rheometry. An advanced rheometric expansion system (ARES, TA Instrument) was used in the oscillatory mode with parallel plate fixtures (8-mm diameter). Dynamic temperature sweep experiments under isochronal conditions were conducted, i.e., the dynamic storage modulus (G') and dynamic loss modulus (G'') were measured at an angular frequency (ω) of 0.1 rad/s during heating. Data acquisition was accomplished with the aid of a microcomputer interfaced with the rheometer. The temperature control was satisfactory to within ±1 °C. All experiments were conducted under a nitrogen atmosphere to preclude oxidative degradation of the samples.

3. Results and Discussion

Effect of the Chemical Structure of Functional Groups on the Dispersion Characteristics of Organoclay in Nanocomposites Based on End-Functionalized Low-Molecular-Weight Polystyrene. Figure 1 gives XRD patterns of organoclay nanocomposites based on neat PSLMW and PSLMW terminated by a −COOH group or a −COONa group. The following observations are worth noting in Figure 1. The XRD patterns indicate that the d spacing of PSLMW/Cloisite 30B nanocomposite is 1.85 nm, which is virtually the same as that of Cloisite 30B, and the d spacing of PSLMW/Cloisite 20A nanocomposite is 1.77 nm, which is slightly smaller than that of Cloisite 20A (2.42 nm). This is not surprising, because no attractive interaction can be expected between neat PS and the surfactant residing at the surface of Cloisite 30B or Cloisite 20A. In Figure 1, we still observe a broad XRD reflection peak having the d spacing of 1.85 nm in both (PSLMW-t-COOH)/Cloisite 30B and (PSLMW-t-COOH)/Cloisite 20A nanocomposites, although the peak height of the XRD patterns for the two nanocomposites is much smaller than that for the PSLMW/Cloisite 30B and PSLMW/Cloisite 20A nanocomposites. This observation seems to suggest that the −COOH group attached to the chain end of PSLMW might not have sufficiently strong attractive interactions with the surfactant residing at the surface of Cloisite 30B and Cloisite 20A,

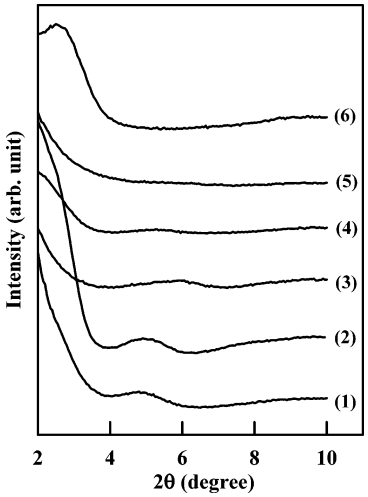

Figure 1. XRD patterns for: (1) PSLMW/Cloisite 30B nanocomposite, (2) PSLMW/Cloisite 20A nanocomposite. (3) (PSLMW-t-COOH)/Cloisite 30B nanocomposite, (4) (PSLMW-t-COOH)/Cloisite 20A nanocomposite, (5) (PSLMW-t-COONa)/Cloisite 30B nanocomposite, and (6) (PSLMW-t-COONa)/Cloisite 20A nanocomposite.

giving rise to a low degree of dispersion of organoclay aggregates in the respective nanocomposites. This can be explained by the following observations. The −COOH group present at the chain end of PSLMW-t-COOH is not expected to have any attractive interactions with the surfactant 2M2HT residing at the surface of Cloisite 20A, while it can potentially form hydrogen bonds with the hydroxyl group in the surfactant MT2EtOH residing at the surface of Cloisite 30B. However, only one −COOH group at the chain end of PSLMW-t-COOH would not be sufficient to form strong attractive interactions with the hydroxyl groups in the surfactant MT2EtOH residing at the surface of Cloisite 30B. The situation would be quite different if many −COOH groups had been present in the entire PSLMW molecule.

Interestingly, in Figure 1, we observe featureless XRD patterns in both (PSLMW-t-COONa)/Cloisite 20A and (PSLMW-t-COONa)/Cloisite 30B nanocomposites. This observation seems to suggest that sufficiently strong attractive interactions might be present between the −COONa group at the chain end of PSLMW and the surfactant (2M2HT or MT2EtOH) residing at the surface of the nanocomposite. We defer our explanation on the origin of strong attractive interactions in the respective nanocomposites until we present more experimental results.

Figure 2 gives TEM images of the nanocomposites based on neat PSLMW and PSLMW terminated by a −COOH group or a −COONa group. In Figure 2, we observe that the degree of dispersion of organoclays, Cloisite 30B and Cloisite 20A, is rather poor in the matrix of neat PSLMW and PSLMW-t-COOH, while both organoclays, Cloisite 30B and Cloisite 20A, are very well dispersed in the matrix of PSLMW-t-COONa.

The results of XRD patterns and TEM images for (PSLMW-t-COOH)/MMT and (PSLMW-t-COONa)/MMT nanocomposites are presented in the Supporting Information, because the results are not particularly interesting. In the TEM images, we observe that MMT aggregates are hardly segregated during solution blending in the matrix of PSLMW-t-COOH or PSLMW-t-COONa. This can easily be understood from the point of view of the structure of MMT.[20,21]

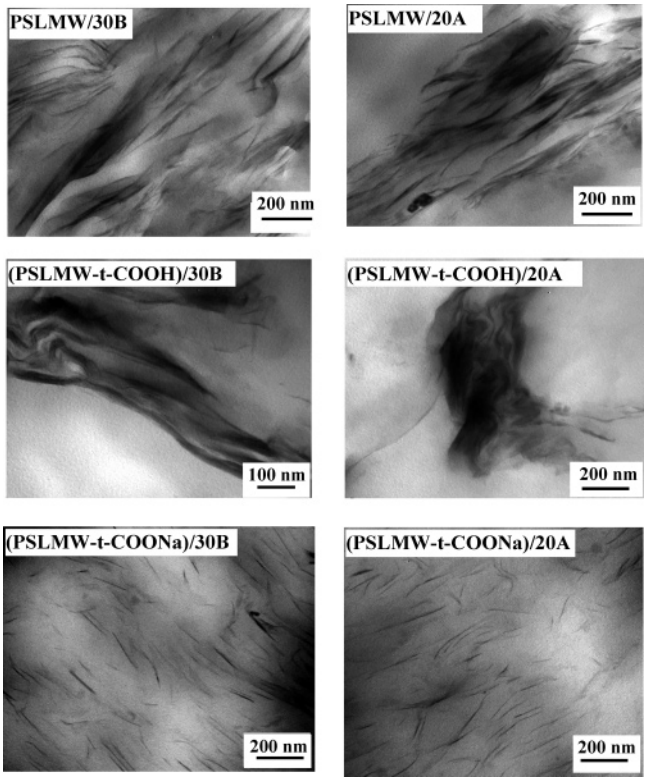

Figure 2. TEM images of PSLMW/Cloisite 30B nanocomposite, PSLMW/Cloisite 20A nanocomposite, (PSLMW-t-COOH)/Cloisite 30B nanocomposite, (PSLMW-t-COOH)/Cloisite 20A nanocomposite, (PSLMW-t-COONa)/Cloisite 30B nanocomposite, and (PSLMW-t-COONa)/Cloisite 20A nanocomposite, in which the dark areas represent organoclay, Cloisite 30B, or Cloisite 20A, and the gray/white areas represent the polymer matrix.

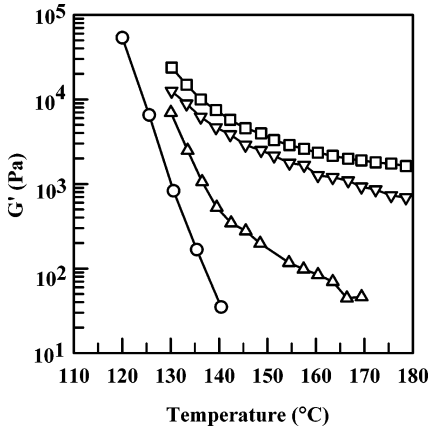

Figure 3. Variations of G' with temperature during the isochronal dynamic temperature sweep experiments at ω = 0.1 rad/s for: (○) PSLMW, (△) PSLMW-t-COONa, (▽) (PSLMW-t-COONa)/Cloisite 20A nanocomposite, and (□) (PSLMW-t-COONa)/Cloisite 30B nanocomposite.

Figure 3 describes the temperature dependence of dynamic storage modulus G' during the isochronal dynamic temperature sweep experiment at an angular frequency (ω) of 0.1 rad/s for PSLMW, PSLMW-t-COONa, (PSLMW-t-COONa)/Cloisite 20A nanocomposite, and (PSLMW-t-COONa)/Cloisite 30B nanocomposite. The following observations are worth noting in Figure 3. Not only is the magnitude of G' for PSLMW-t-COONa much larger than that for neat PSLMW, but also the values of G' for PSLMW-t-COONa decrease slowly, as compared to the values of G' for neat PSLMW,

with increasing temperature. We attribute this observation to the formation of ionic clusters in PSLMW-t-COONa. It has been reported[22,23] that ionic groups attached to the chains of an organic polymer form quadruplets, sextuplets, and higher aggregates (multiplets), leading to clusters, which then reduce the mobility of the polymer chains and act like cross-links or reinforcing filler particles. Further, it has been reported[24] that the ionic clusters are very stable at elevated temperatures, giving rise to a slow decrease in elastic modulus with increasing temperature. It is interesting to observe in Figure 3 that the values of G' for the (PSLMW-t-COONa)/Cloisite 30B nanocomposite decrease extremely slowly with increasing temperature from 130 to 180 °C, and the value of G' at 180 °C for the nanocomposite is about 2 orders of magnitude greater than that for PSLMW-t-COONa. Similar results can be made for the (PSLMW-t-COONa)/Cloisite 20A nanocomposite from Figure 3. We attribute the unusual temperature dependence of G' to the presence of ionic interactions between the $-COO^-$ at the chain end of PSLMW and the N^+ present at the surface of the organoclays, Cloisite 30B or Cloisite 20A. Note that the surfactant MT2EtOH residing at the surface of Cloisite 30B, and also the surfactant 2M2HT residing at the surface of Cloisite 20A, have quaternary ammonium salt having alkyl bonds to a nitrogen atom, and the nitrogen atom bears a full positive charge. It is well established that the ionic interaction is much stronger, although not as strong as covalent bonding, than hydrogen bonding. Earlier, Eisenberg and co-workers[25−28] utilized ionic interactions to enhance the miscibility of immiscible polymer blends. Then it seems very reasonable to conclude that ionic interactions between negatively charged $-COO^-$ at the chain end of PSLMW and the positively charged N^+ in the surfactant (MT2EtOH in Cloisite 30B and 2M2HT in Cloisite 20A) enhanced the compatibility between PSLMW-t-COONa and organoclay (Cloisite 30B or Cloisite 20A) and, thus, gave rise to a high degree of dispersion of organoclay aggregates in the matrix of PSLMW-t-COONa (see the TEM images given in Figure 2). Here, we use the term "a high degree of dispersion" in the qualitative sense because it is very difficult, if not impossible, to describe quantitatively the degree of dispersion (low, medium, or high) from the TEM images given in Figure 2.

We measured the molecular weight and its distribution of (PSLMW-t-COONa)/Cloisite 30B nanocomposite before and after the isochronal dynamic sweep experiment. We have found that the molecular weights of the specimens are virtually identical before and after the rheological measurement, as given in the GPC traces presented in the Supporting Information.

Figure 4 gives log G' versus log G'' plots for (PSLMW-t-COONa)/Cloisite 30B nanocomposites at various temperatures ranging from 140 to 175 °C. It should be mentioned that Figure 4 was prepared from the experimental results of dynamic frequency sweep experiments, with the plots of log G' versus log ω and log G'' versus log ω for the (PSLMW-t-COONa)/Cloisite 30B nanocomposite at various temperatures being presented in the Supporting Information. In Figure 4, we observe that the log G' versus log G'' plots for the (PSLMW-t-COONa)/Cloisite 30B nanocomposite are virtually independent of temperature, suggesting that the morphological state of the nanocomposite remains constant over the entire range of temperatures investigated. Notice

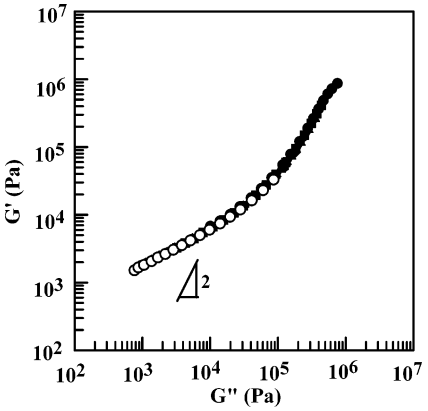

Figure 4. Plots of log G' versus log G'' for (PSLMW-t-COONa)/Cloisite 30B nanocomposite at various temperatures (°C): (●) 140, (■) 150, (▲) 155, (▼) 160, (◆)165, (⬢) 170, and (○) 175.

in Figure 4 that, in the terminal region, the slope of log G' versus log G'' plots is much less than 2, a signature of the presence of attractive interactions between the N^+ ion in the surfactant MT2EtOH residing at the surface of Cloisite 30B and the $-COO^-$ ion at the chain end of the matrix PSLMW-t-COONa.

Earlier, on the basis of the Doi−Edwards molecular viscoelasticity theory,[29] Han and co-workers[30−32] have shown that the slope of log G' versus log G'' plots in the terminal region is 2 for an entangled flexible homopolymer:

$$\log G' = 2 \log G'' + \log (6/5G_N^o) \qquad (1)$$

where G_N^o is the plateau modulus. The validity of eq 1 has been supported by experiments on flexible homopolymer,[30,33] miscible polymer blends,[34,35] block copolymers in the disordered state,[36−39] and liquid crystalline polymers in the isotropic state.[40,41]

To directly probe evidence of ionic interactions between the negatively charged $-COO^-$ at the chain end of PSLMW and the positively charged N^+ in the surfactant MT2EtOH residing at the surface of Cloisite 30B, we washed the (PSLMW-t-COONa)/Cloisite 30B nanocomposite several times with toluene, followed by drying, and then ran Fourier transform infrared (FTIR) spectroscopy of the specimen. Figure 5 gives FTIR spectra for (a) PSLMW-t-COONa, (b) Cloisite 30B, (c) washed (PSLMW-t-COOH)/Cloisite 30B nanocomposite, and (d) washed (PSLMW-t-COONa)/Cloisite 30B nanocomposite. The following observations are worth noting in Figure 5. As expected, no absorption band appears at the wavenumber of 3620 cm^{-1} for PSLMW-t-COONa. However, two new absorption bands at the wavenumbers 3620 and 1500 cm^{-1} appear in Cloisite 30B and in the two nanocomposites. This is due to the presence of $-OH$ groups in the surfactant MT2EtOH residing at the surface of Cloisite 30B. To facilitate our discussion here, an inset is given in Figure 5 showing the absorption bands at wavenumbers ranging from 1200 to 1800 cm^{-1}. It is clearly seen from the inset that an additional absorption band appears at 1570 cm^{-1} for the (PSLMW-t-COONa)/Cloisite 30B nanocomposite; otherwise, the absorption bands are identical for both the (PSLMW-t-COONa)/Cloisite 30B and (PSLMW-t-COOH)/Cloisite 30B nanocomposites.

Earlier, Yano and co-workers[42,43] conducted infrared spectroscopy studies of the binary blends of sodium and

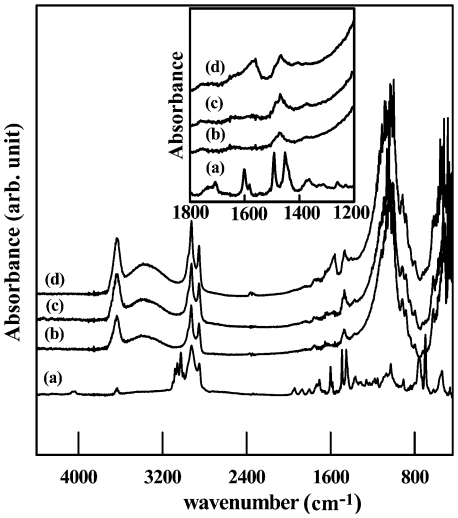

Figure 5. FTIR spectra for: (a) PSLMW-t-COONa, (b) Cloisite 30B, (c) (PSLMW-t-COOH)/Cloisite 30B nanocomposite, and (d) (PSLMW-t-COONa)/Cloisite 30B nanocomposite.

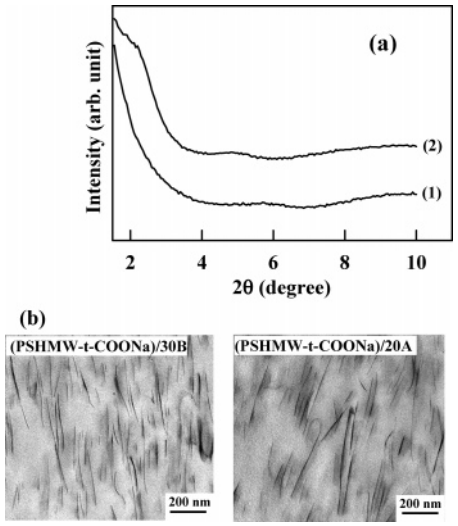

Figure 6. (a) XRD patterns for (1) (PSHMW-t-COONa)/Cloisite 30B nanocomposite and (2) (PSHMW-t-COONa)/Cloisite 20A nanocomposite; (b) TEM images of (PSHMW-t-COONa)/Cloisite 30B nanocomposite and (PSHMW-t-COONa)/Cloisite 20A nanocomposite, in which the dark areas represent organoclay, Cloisite 30B, or Cloisite 20A, and the gray/white areas represent the polymer matrix.

zinc salt ionomers of poly(ethylene-*co*-methacrylate) (PEMMA) and observed the appearance of a new asymmetric carboxylate stretching band at 1569 cm^{-1}, which is very close to the wavelength 1570 cm^{-1} observed in our study, shown in Figure 5. They assigned the appearance of a stretching band 1569 cm^{-1} to carboxylate groups bridging sodium and zinc cations. Thus, we conclude that the appearance of a new absorption peak at 1570 cm^{-1} in Figure 5 is due to the ionic interactions between the negatively charged $-COO^-$ at the chain end of PSLMW-t-COONa and the positively charged quaternary ammonium in the surfactant (2M2HT or MT2EtOH) residing at the surface of organoclay (Cloisite 20A or Cloisite 30B).

Effect of Molecular Weight of End-Functionalized Polystyrene on the Dispersion Characteristics of Organoclay in Nanocomposites. Figure 6 describes (a) XRD patterns and (b) TEM images of organoclay nanocomposites based on an end-functionalized high-molecular-weight PSHMW-t-COONa. It can be seen in Figure 6a that the XRD patterns of both (PSHMW-t-COONa)/Cloisite 30B and (PSHMW-t-COONa)/Cloisite 20A nanocomposites show a very weak and broad peak at 2θ of 4−6°. Compare the XRD patterns for the (PSHMW-t-COONa)/Cloisite 30B and (PSHMW-t-COONa)/Cloisite 20A nanocomposites given in Figure 6a with those for the (PSLMW-t-COONa)/Cloisite 30B and (PSLMW-t-COONa)/Cloisite 20A nanocomposites given in Figure 1. The XRD patterns given in Figure 1 for the (PSLMW-t-COONa)/Cloisite 30B and (PSLMW-t-COONa)/Cloisite 20A nanocomposites are featureless, suggesting that the organoclay aggregates in the nanocomposites based on PSLMW may be dispersed better than those based on PSHMW. This observation is supported by the TEM images given in Figure 6b, as compared to the TEM images given in Figure 2, in that the aggregates of organoclays, Cloisite 30B and Cloisite 20A, appear to be slightly better dispersed in the matrix of PSLMW-t-COONa than in the matrix of PSHMW-t-COONa.

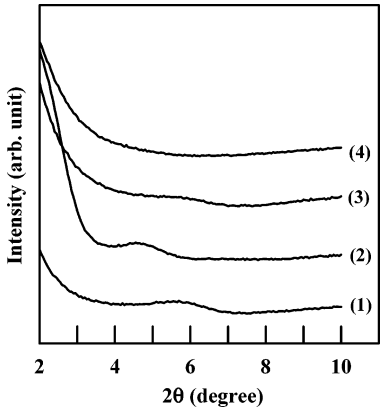

Figure 7. XRD patterns for: (1) (IS-t-COOH)/Cloisite 30B nanocomposite, (2) (IS-t-COOH)/Cloisite 20A nanocomposite, (3) (IS-t-COONa)/Cloisite 30B nanocomposite, and (4) (IS-t-COONa)/Cloisite 20A nanocomposite.

The above observation seems to indicate that the molecular weight of the polymer matrix (PSLMW versus PSHMW) has some influence on the dispersion characteristics of organoclay aggregates in nanocomposites. The above experimental observations can be interpreted as follows. The concentration of $-COO^-$ ions at the chain end of PSLMW-t-COONa is higher than that at the chain end of PSHMW-t-COONa. Specifically, for 100 g of nanocomposite containing 5 wt % of organoclay, it is estimated that 4.5 mequiv cations are present in the (PSLMW-t-COONa)/Cloisite 30B nanocomposite, and 4.75 mequiv cations are present in the (PSLMW-t-COONa)/Cloisite 20A nanocomposites.[44] On the other hand, it is estimated that 3.5 mequiv $-COO^-$ ions are present in the PSLMW ionomer, while 1.35 mequiv $-COO^-$ ions are present in the PSHMW ionomer (see Table 1 for the molecular weights of PSLMW and PSHMW). Therefore, the (PSLMW-t-COONa)/Cloisite 30B nanocomposite is expected to have a higher degree of ionic interactions than the (PSHMW-t-COONa)/Cloisite 30B nanocomposite, which would lead to an enhanced degree of organoclay dispersion.

Effect of End-Functionalization of SI Diblock Copolymer on the Dispersion Characteristics of Organoclay Nanocomposites. Figure 7 gives XRD patterns of organoclay nanocomposites based on IS-t-COOH or IS-t-COONa, in which the functional groups

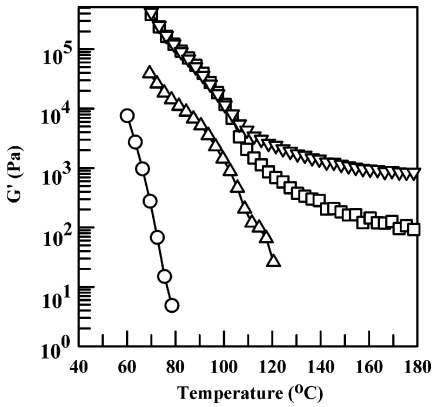

Figure 8. Variations of G' with temperature during the isochronal dynamic temperature sweep experiments at ω = 0.1 rad/s for: (○) SI-2, (△) IS-t-COONa, (□) (IS-t-COONa)/Cloisite 30B nanocomposite, and (▽) (IS-t-COONa)/Cloisite 20A nanocomposite.

−COOH or −COONa is attached to the chain end of PS block of an SI diblock copolymer (SI-2). The following observations are worth noting in Figure 7. (i) The XRD patterns of (IS-t-COOH)/Cloisite 30B nanocomposite show a reflection peak at $2\theta = 5.8°$ (the d spacing of 1.47 nm), and the XRD patterns of (IS-t-COOH)/Cloisite 20A nanocomposite show a conspicuous reflection peak at $2\theta = 4.6°$ (the d spacing of 1.85 nm), suggesting that both nanocomposites would have a low degree of dispersion of organoclay aggregates. (ii) The XRD patterns of (IS-t-COONa)/Cloisite 30B nanocomposite show a very mild reflection peak, while the XRD patterns of (IS-t-COONa)/Cloisite 20A nanocomposite show featureless XRD patterns over the entire range of 2θ angles investigated. The above observation seems to suggest that the (IS-t-COONa)/Cloisite 20A nanocomposite might have a slightly higher degree of dispersion of organoclay aggregates than the (IS-t-COONa)/Cloisite 30B nanocomposite.

Figure 8 describes the temperature dependence of G' during isochronal dynamic temperature sweep experiments for neat SI diblock copolymer SI-2 (○), IS-t-COONa (△), (IS-t-COONa)/Cloisite 30B nanocomposite (□), and (IS-t-COONa)/Cloisite 20A nanocomposite (▽). It has been suggested[45] that such plots can be used to determine the order−disorder transition (ODT) temperature (T_{ODT}) of a block copolymer by identifying the temperature at which values of G' begin to drop precipitously. The following observations are worth noting in Figure 8. (i) Values of G' for the neat block copolymer SI-2 decrease steadily with increasing temperature over the entire range of temperatures investigated from 60 to 80 °C, suggesting that SI-2 is a disordered block copolymer. (ii) At 80 °C, the value of G' for the end-functionalized diblock copolymer IS-t-COONa is about 3 orders of magnitude larger than that for the neat diblock copolymer SI-2. Notice further from Figure 8 that values of G' for IS-t-COONa initially decrease slowly with increasing temperature from 70 to ca. 90 °C, and then more rapidly with further increase in temperature. Earlier, Choi and Han[18] reported a very large increase in G' when a homogeneous polystyrene-*block*-polyisoprene-*block*-polystyrene (SIS triblock) copolymer was end-functionalized with a −COONa group, which then induced microphase separation in the SIS triblock copolymer. On the basis of such experimental observations, we tentatively conclude that IS-t-COONa might have microdomains. (iii) Values of G' for both

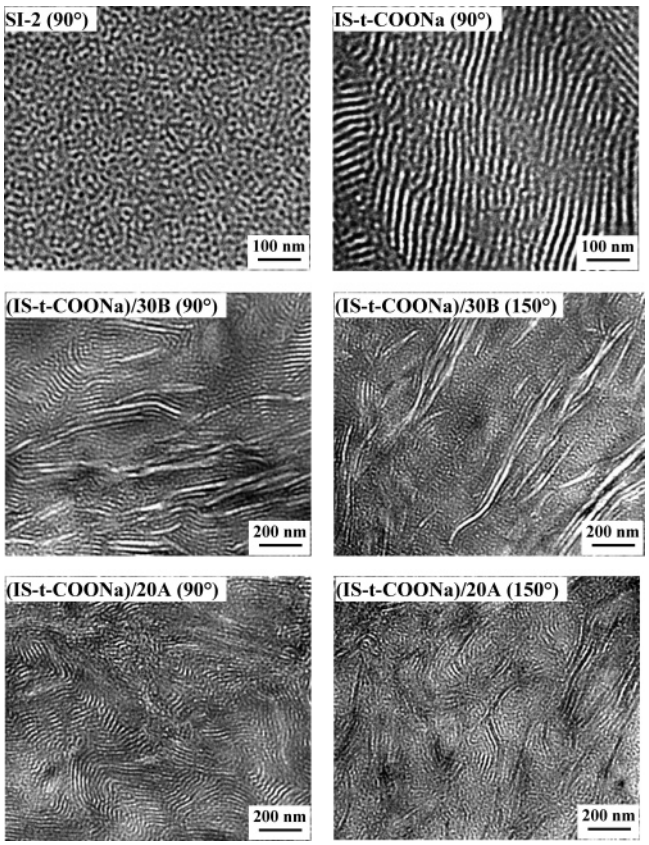

Figure 9. TEM images of (i) SI-2 at 90 °C, (ii) IS-t-COONa at 90 °C, (iii) (IS-t-COONa)/Cloisite 30B nanocomposite at 90 °C, (iv) (IS-t-COONa)/Cloisite 30B nanocomposite at 150 °C, (v) (IS-t-COONa)/Cloisite 20A nanocomposite at 90 °C, and (vi) (IS-t-COONa)/Cloisite 20A nanocomposite at 150 °C. Specimen was first annealed at 90 °C for 24 h or at 150 °C for 6 h and then stained with osmium tetroxide, followed by a rapid quench in ice water.

(IS-t-COONa)/Cloisite 30B and (IS-t-COONa)/Cloisite 20A nanocomposites initially decrease rapidly with increasing temperature to ca. 105 °C, and then very slowly as the temperature is increased further to ca. 180 °C. It is very interesting to observe in Figure 8 that values of G' for the (IS-t-COONa)/Cloisite 30B and (IS-t-COONa)/Cloisite 20A nanocomposites at 180 °C are still very large, suggesting the possibility that the block copolymer matrix IS-t-COONa in the respective nanocomposites might still have microdomains. Such a possibility, if it is borne out to be true, may be attributable to the formation of ionic clusters between the $-COO^-$ at the chain end of PS block of SI-2 and the positively charged N^+ in the surfactant (MT2EtOH or 2M2HT) residing at the surface of organoclay (Cloisite 30B or Cloisite 20A).

Figure 9 gives TEM images of neat SI diblock copolymer SI-2 at 90 °C, IS-t-COONa at 90 °C, and (IS-t-COONa)/Cloisite 30B and (IS-t-COONa)/Cloisite 20A nanocomposites at 90 and 150 °C. The following observations are worth noting in Figure 9. (i) The TEM image of SI-2 at 90 °C shows structures that resemble very much the liquidlike disordered structure of a nearly symmetric block copolymer reported by Sakamoto and Hashimoto.[46] Note that SI-2 is a nearly symmetric block copolymer. It has been reported[47,48] that a nearly symmetric disordered block copolymer exhibits the temperature dependence of storage modulus, very similar to that shown in Figure 8 for SI-2 (the symbol ○),

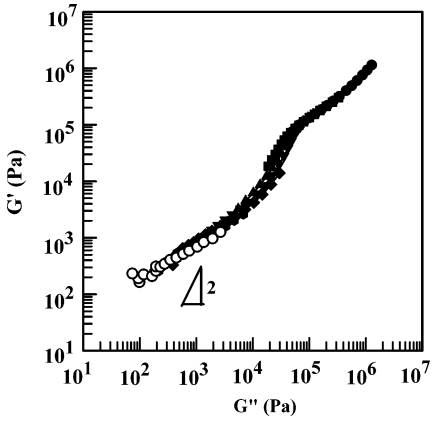

Figure 10. Plots of log G' versus log G'' for (IS-t-COONa)/Cloisite 30B nanocomposite at various temperatures (°C): (●) 80, (■) 90, (▲) 100, (▼) 110, (◆)130, (⬢) 150, and (○) 170.

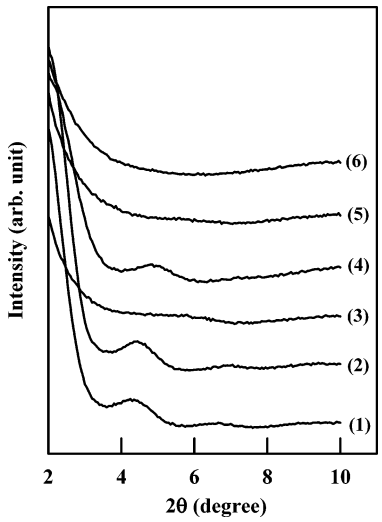

Figure 11. XRD patterns for: (1) (SI-1)/Cloisite 30B nanocomposite, (2) (SI-1)/Cloisite 20A nanocomposite, (3) (SI-t-COOH)/Cloisite 30B nanocomposite, (4) (SI-t-COOH)/Cloisite 20A nanocomposite, (5) (SI-t-COONa)/Cloisite 30B nanocomposite, and (6) (SI-t-COONa)/Cloisite 20A nanocomposite.

having a liquidlike disordered structure, and also very similar to that shown in Figure 3 for neat polystyrene PSLMW (the symbol ○). Therefore, SI-2, having a liquidlike disordered structure, can be regarded as being a disordered block copolymer. We then conclude that there is a direct correlation between the liquidlike disordered structure of SI-2 (TEM image for SI-2 in Figure 9) and its temperature dependence of a storage modulus (the symbol ○ in Figure 8). (ii) The TEM image of IS-t-COONa at 90 °C shows lamellar microdomains, in which the dark areas represent the PI phase that was stained by osmium tetroxide, and the bright areas represent the PS phase. What is significant in the TEM image of IS-t-COONa lies in that microphase separation has been induced by attaching a −COONa group at the chain end of PS block of a homogeneous SI diblock copolymer, SI-2. Note that SI-2 is a nearly symmetric diblock copolymer (see Table 1 for the block compositions). (iii) The TEM images of (IS-t-COONa)/Cloisite 30B and (IS-t-COONa)/Cloisite 20A nanocomposites at 90 °C show a coexistence of the microdomains of the matrix phase IS-t-COONa and the organoclay (Cloisite 30B or Cloisite 20A). Of particular note is that, at 150 °C, the block copolymer matrix IS-t-COONa in the (IS-t-COONa)/Cloisite 30B and (IS-t-COONa)/Cloisite 20A nanocomposites still retain microdomains, although they do not appear to be perfectly aligned lamellae. In other words, the lamellar microdomain structure of IS-t-COONa in the nanocomposite seems to have been modified somewhat in the presence of organoclay, Cloisite 30B or Cloisite 20A. Recent studies[49,50] have noted similar observations. The presence of microdomains of the block copolymer matrix IS-t-COONa at 150 °C supports the observation made above from Figure 8 that the ionic interactions between the $-COO^-$ at the chain end of PS block of SI-2 and the positively charged N^+ in the surfactant (MT2EtOH or 2M2HT) residing at the surface of organoclay (Cloisite 30B or Cloisite 20A) were sufficiently strong, so as to not allow the microdomains of IS-t-COONa to disappear at a temperature as high as 150 °C (and most likely even at 180 °C on the basis of Figure 8).

Figure 10 gives log G' versus log G'' plots for (IS-t-COONa)/Cloisite 30B nanocomposites at various temperatures ranging from 80 to 170 °C. Note that Figure 10 was prepared from the experimental results of dynamic frequency sweep experiments, and plots of log G' versus log ω and log G'' versus log ω for the (IS-t-COONa)/Cloisite 30B nanocomposite at various temperatures are presented in the Supporting Information. In Figure 10, we observe that the log G' versus log G'' plots for the (IS-t-COONa)/Cloisite 30B nanocomposite are slightly dependent upon temperature, suggesting that the morphological state of the nanocomposite did not change that much over the entire range of temperatures investigated. Notice in Figure 10 that, in the terminal region, the slope of the log G' versus log G'' plots is far less than 2, indicative of the presence of attractive interactions between the N^+ ion in the surfactant MT2EtOH residing at the surface of Cloisite 30B and the $-COO^-$ ion at the chain end of the matrix IS-t-COONa. Had there been no ionic interactions in the (IS-t-COONa)/Cloisite 30B nanocomposite, the slope of log G' versus log G'' plots in the terminal region would have been close to 2.

Figure 11 shows XRD patterns of nanocomposites based on neat SI diblock copolymer SI-1, SI-t-COOH, or SI-t-COONa, in which functional groups, −COOH or −COONa, are attached to the chain end of PI block of SI-1. The following observations are worth noting in Figure 11. (i) The XRD patterns of SI/Cloisite 30B nanocomposite show a broad reflection peak at $2\theta = 4.6°$ (the d spacing of 1.85 nm), and SI/Cloisite 20A nanocomposite's XRD patterns show a broad reflection peak at $2\theta = 4.8°$ (the d spacing of 1.77 nm). Notice that the shape of the XRD patterns for SI/Cloisite 30B and SI/Cloisite 20A nanocomposites shown in Figure 11 is very similar to that for PSLMW/Cloisite 30B and PSLMW/Cloisite 20A nanocomposites (see Figure 1). Thus, we can tentatively conclude that both SI/Cloisite 30B and SI/Cloisite 20A nanocomposites would have a low degree of dispersion of organoclay aggregates. This is not surprising because no attractive interaction is expected between the SI block and the surfactant (MT2EtOH or 2M2HT) residing at the surface of the organoclay employed. (ii) The XRD pattern of (SI-t-COOH)/Cloisite 30B nanocomposite shows a very mild reflection peak, while the XRD pattern of (SI-t-COOH)/Cloisite 20A nanocomposite shows a conspicuous reflection peak at $2\theta = 5.0°$ (the d spacing of 1.70 nm). This observation leads us to conclude that (SI-t-COOH)/Cloisite 30B nanocomposite might have a higher degree of dispersion of organoclay aggregates than (SI-t-COOH)/

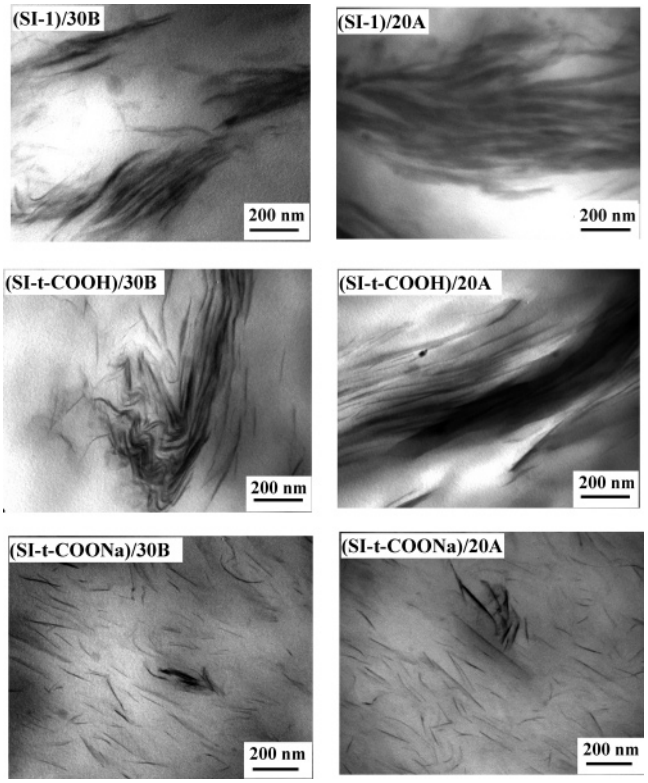

Figure 12. TEM images at room temperature of (SI-1)/Cloisite 30B nanocomposite, (SI-1)/Cloisite 20A nanocomposite, (SI-t-COOH)/Cloisite 30B nanocomposite, (SI-t-COOH)/Cloisite 20A nanocomposite, (SI-t-COONa)/Cloisite 30B nanocomposite, and (SI-t-COONa)/Cloisite 20A nanocomposite, in which the dark areas represent organoclay, Cloisite 20A, or Cloisite 30B, and the gray/white areas represent the polymer matrix. The specimens were not stained by osmium tetroxide.

Cloisite 20A nanocomposite. Again, this observation seems reasonable from the point of view that the −COOH group at the chain end of the PI block of SI-1 is expected to have very weak interactions, if any, with the hydroxyl groups in the surfactant MT2EtOH residing at the surface of Cloisite 30B, while no attractive interaction is expected between the −COOH group at the chain end of the PI block of SI-1 and the surfactant 2M2HT residing at the surface of Cloisite 20A. (iii) Both (SI-t-COONa)/Cloisite 30B and (SI-t-COONa)/Cloisite 20A nanocomposites show featureless XRD patterns over the entire range of 2θ angles investigated, suggesting that a very high degree of dispersion of organoclay aggregates is expected in the matrix of SI-t-COONa for the respective nanocomposites. This observation is very similar to that made above for the (PSLMW-t-COONa)/Cloisite 30B nanocomposite (see Figure 1) and (IS-t-COONa)/Cloisite 20A nanocomposite (see Figure 7).

Figure 12 gives TEM images of the nanocomposites based on SI-1, SI-t-COOH, or SI-t-COONa. To help observe clearly the state of dispersion of organoclay aggregates in the matrix phase, the block copolymer in the respective nanocomposites were not stained with osmium tetroxide. Thus, the white/gray areas represent the block copolymer matrix phase, and the dark areas represent organoclay. It can be seen in Figure 12 that the nanocomposites based on SI-1 and SI-t-COOH have very poor dispersions of organoclay aggregates, whereas the aggregates of Cloisite 30B and Cloisite 20A are very well dispersed in the matrix of SI-t-COONa. This observation is consistent with that made above from the

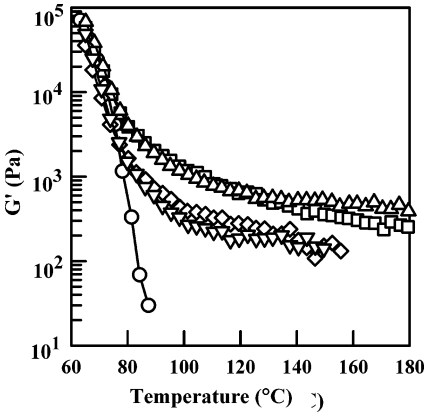

Figure 13. Variations of G' with temperature during the isochronal dynamic temperature sweep experiments at ω = 0.1 rad/s for: (○) SI-t-COONa, (▽) (SI-t-COOH)/Cloisite 30B nanocomposite, (◇) (SI-t-COOH)/Cloisite 20A nanocomposite, (△) (SI-t-COONa)/Cloisite 30B nanocomposite, and (□) (SI-t-COONa)/Cloisite 20A nanocomposite.

XRD patterns given in Figure 11. Again, we attribute this observation to the presence of ionic interactions between the negatively charged $-COO^-$ present at the chain end of the PI block of an SI-t-COONa and the positively charged N^+ in the surfactant (MT2EtOH or 2M2HT) residing at the surface of organoclay (Cloisite 30B or Cloisite 20A). On the other hand, the rather poor dispersion of organoclay aggregates in the matrix of SI-1 and SI-t-COOH is due to the absence (or insufficient) attractive interaction between the polymer matrix and the surfactant, MT2EtOH or 2M2HT, residing at the surface of the respective organoclays, Cloisite 30B and Cloisite20A.

Figure 13 describes the temperature dependence of G' during isochronal dynamic temperature sweep experiments for SI-t-COONa (○), (SI-t-COOH)/Cloisite 30B nanocomposite (▽), (SI-t-COOH)/Cloisite 20A nanocomposite (◇), (SI-t-COONa)/Cloisite 30B nanocomposite (△), and (SI-t-COONa)/Cloisite 20A nanocomposite (□). The following observations are worth noting in Figure 13. (i) Values of G' for SI-t-COONa decrease steadily with increasing temperature over the entire range of temperatures investigated from 60 to 90 °C, suggesting that the end-functionalized block copolymer SI-t-COONa has no microdomains. (ii) Values of G' for the (SI-t-COOH)/Cloisite 30B and (SI-t-COOH)/Cloisite 20A nanocomposites initially decrease rapidly as the temperature is increased from 60 to ca. 80 °C, and then at a much slower rate as the temperature is increased further to 160 °C. It is interesting to observe in Figure 13 that values of G' for the nanocomposites are still substantial even at 150 °C, suggesting that, in the presence of organoclay (Cloisite 30B or Cloisite 20A), the block copolymer matrix SI-t-COOH in the respective nanocomposites might still retain microdomains. The temperature dependence of G' for the (SI-t-COONa)/Cloisite 30B and (SI-t-COONa)/Cloisite 20A nanocomposites is similar to that for the (SI-t-COOH)/Cloisite 30B and (SI-t-COOH)/Cloisite 20A nanocomposites, but the magnitude of G' at 100−150 °C is much larger for the nanocomposites based on SI-t-COONa than that for the nanocomposites based on SI-t-COOH. This observation seems to suggest that the ionic interactions between the −COONa group at the chain end of PI block in the SI-t-COONa and the surfactant (MT2EtOH or 2M2HT) residing at the surface of organoclay (Cloisite 30B or Cloisite 20A) are much stronger than the interactions

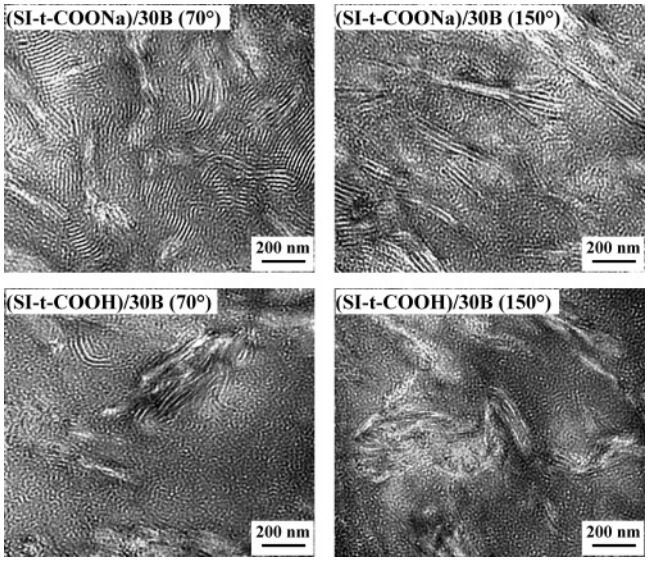

Figure 14. TEM images of (SI-t-COONa)/Cloisite 30B nanocomposite at 70 and at 150 °C (in the upper panel), and TEM images of (SI-t-COOH)/Cloisite 30B nanocomposite at 70 and 150 °C (in the lower panel). Specimen was first annealed at 70 °C for 24 h or at 150 °C for 6 h and then stained with osmium tetroxide, followed by a rapid quench in ice water.

between the −COOH group at the chain end of PI block in the SI-t-COOH and the surfactant. As pointed out above, the interactions between the −COOH group in SI-t-COOH and the surfactant MT2EtOH residing at the surface of organoclay Cloisite 30B would be relatively weak.

The upper panel of Figure 14 gives TEM images of (SI-t-COONa)/Cloisite 30B nanocomposite at 70 and 150 °C, and the lower panel of Figure 14 gives TEM images of (SI-t-COOH)/Cloisite 30B nanocomposite at 70 and 150 °C, for which each specimen was first stained with osmium tetroxide, then annealed at 70 °C for 6 h and at 150 °C for 2 h, followed by rapid quenching in ice water. In Figure 14, we observe that, at 70 °C, the lamellar microdomains of SI-t-COONa and the organoclay Cloisite 30B coexist, indicating that microdomain separation was induced, via ionic interaction between the $-COO^-$ group at the chain end of PI block in SI-t-COONa and the surfactant MT2EtOH residing at the surface of Cloisite 30B, when a disordered (homogeneous) diblock copolymer SI-t-COONa was mixed with organoclay Cloisite 30B. Note that, according to the results of the isochronal dynamic temperature sweep experiment given in Figure 13, SI-t-COONa is a disordered block copolymer. Interestingly, as the temperature is increased to 150 °C, the (SI-t-COONa)/Cloisite 30B nanocomposite still retains microdomains of the matrix phase SI-t-COONa in the presence of exfoliated organoclay Cloisite 30B. However, the microdomain structure of SI-t-COONa at 150 °C does not look the same as that at 70 °C, i.e., at 150 °C, little lamellar microdomain structure is seen in the TEM image of (SI-t-COONa)/Cloisite 30B nanocomposite, while the aggregates of organoclay Cloisite 30B are well dispersed in the block copolymer matrix. This observation is very similar to that made above in reference to the TEM image of (IS-t-COONa)/Cloisite 30B nanocomposite given in Figure 9.

Plots of log G' versus log G'' plots are given in Figure 15 for (SI-t-COONa)/Cloisite 30B nanocomposite at various temperatures ranging from 80 to 180 °C, and

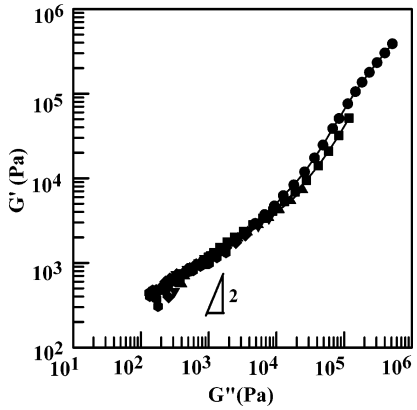

Figure 15. Plots of log G' versus log G'' for (SI-t-COONa)/Cloisite 30B nanocomposite at various temperatures (°C): (●) 80, (■) 100, (▲) 120, (▼) 140, (◆)160, and (⬢) 180.

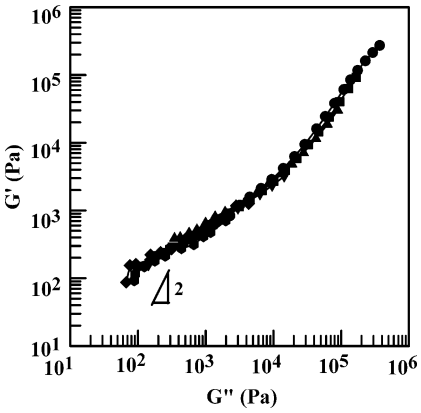

Figure 16. Plots of log G' versus log G'' for (SI-t-COOH)/Cloisite 30B nanocomposite at various temperatures (°C): (●) 80, (■) 90, (▲) 100, (▼) 120, (◆)140, and (⬢) 160.

similar plots are given in Figure 16 for (SI-t-COOH)/Cloisite 30B nanocomposite at various temperatures ranging from 80 to 160 °C. Plots of log G' versus log ω and log G'' versus log ω for both (SI-t-COONa)/Cloisite 30B and (SI-t-COOH)/Cloisite 30B nanocomposites at various temperatures are presented in the Supporting Information. From Figures 15 and 16, we can conclude that specific interactions exist in the respective nanocomposites. Again, had there been no specific interactions in the respective nanocomposites, the slope of log G' versus log G'' plots in the terminal region would be close to 2.

5. Concluding Remarks

In this paper, we have shown that the nanocomposites based on polystyrene or SI diblock copolymer, each being end-functionalized with a −COONa group, have a very high degree of exfoliation of organoclay aggregates, as determined by XRD (see Figures 1, 7, and 11) and TEM (see Figures 2, 9, 12, and 14). Two organoclays were employed to prepare nanocomposites: Cloisite 20A, having methyl, hydrogenated tallow, quaternary ammonium chloride (2M2HT) as surfactant, and Cloisite 30B, having methyl, tallow, bis-2-hydroxyethyl, quaternary ammonium chloride (MT2EtOH) as surfactant. We have found *little* or *no* difference between Cloisite 20A and Cloisite 30B in achieving a very high degree of dispersion (exfoliation) of organoclay aggregates when the nanocomposites were based on a polymer matrix that had a −COONa group at chain end. We attribute the exfoliation of organoclay (Cloisite 20A or Cloisite

30B) to the presence of ionic interactions between the negatively charged $-COO^-$ at the chain end of polymer matrix and the positively charged N^+ in the surfactant (MT2EtOH or 2M2HT) residing at the surface of the organoclay. In our previous study,[15] we observed that the aggregates of organoclay Cloisite 30B were very well dispersed (exfoliated), while the aggregates of organoclay Cloisite 20A were poorly dispersed (intercalated), when each of the two organoclays was mixed with a polyisoprene-*block*-polystyrene-*block*-hydroxylated polybutadiene (ISBOH triblock) copolymer. We attributed the exfoliation of the aggregates of organoclay Cloisite 30B in the matrix of ISBOH triblock copolymer to the presence of hydrogen bonds formed between the hydroxyl groups in the surfactant MT2EtOH residing at the surface of Cloisite 30B and the hydroxyl group in the PBOH block of ISBOH. On the other hand, the aggregates of organoclay Cloisite 20A were only intercalated in the matrix of ISBOH block copolymer because the surfactant 2M2HT residing at the surface of Cloisite 20A did not have any functional group that could form hydrogen bonds with the matrix of ISBOH. Comparison of the present study with our previous study[15] points out that different types of specific interactions (e.g., ionic interaction, hydrogen bonding) prevail, depending upon the chemical structures of polymer matrix and the surfactant residing at the surface of an organoclay, and give rise to an exfoliated structure of organoclay aggregates in nanocomposites. Nevertheless, both studies indicate that strong attractive interactions between an organoclay and a polymer matrix are necessary in order to obtain exfoliation of organoclay aggregates in nanocomposites.

What is considered to be remarkable from the present study is that end functionalization of a polystyrene or an SI diblock copolymer is sufficient to achieve a very high degree of dispersion (exfoliation) of organoclay aggregates in a nanocomposite when appropriate functionalities exist in the polymer matrix and organoclay. The present study demonstrates that ionic association is much more effective in achieving exfoliated structure of organoclay aggregates than hydrogen bonding, confirming the general notion that the strength of ionic association is much greater than that of hydrogen bonding. Specifically, we have found that the organoclay nanocomposites based on PS or SI diblock copolymer, each being end-functionalized with a $-COOH$ group, yielded only intercalation of organoclay aggregates, whereas the organoclay nanocomposites based on PS or SI diblock copolymer, each being end functionalized with a $-COONa$ group, yielded exfoliation of organoclay aggregates in nanocomposites. One might expect that the $-COOH$ group at the chain end of PS or SI diblock copolymer can form hydrogen bonds with the $-OH$ groups in the surfactant MT2EtOH residing at the surface of organoclay Cloisite 30B. But, our efforts to find, via FTIR spectroscopy, evidence of hydrogen bonds in the (PSLMW-t-COOH)/Cloisite 30B and (SI-t-COOH)/Cloisite 30B nanocomposites were unsuccessful. Thus, we conclude that no or extremely weak hydrogen bonds might have been formed in the respective nanocomposites, suggesting that the presence of only one $-COOH$ group at the chain end of homopolymer PS and SI diblock copolymer is not sufficient to give rise to strong hydrogen bonds with the $-OH$ groups in the surfactant MT2EtOH residing at the surface of organoclay Cloisite 30B.

It is worth mentioning that, previously, Chisholm et al.[51] reported on the effectiveness of an ionomer on exfoliation of organoclay aggregates when poly(butylene terephthalate) (PBT) functionalized with sodium sulfonate ($-SO_3Na$) was melt blended with a chemically modified montmorillonite (Clayton HY, Southern Clay Products). The surfactant treated on the surface of natural clay was dimethyldihydrogenatedtallow alkyl quaternary ammonium, which is virtually the same as the surfactant 2M2HT residing at the surface of Cloisite 20A. They concluded that the experimentally observed exfoliation of organoclay aggregates was due to ionic interactions between the negatively charged $-SO_3^-$ ion in the PBT-ionomer and the positively charged N^+ ion in the surfactant (R_4N^+) residing at the surface of organoclay Clayton HY. Their conclusion is very similar to our conclusion made from this study. However, the difference between the two studies lies in the positions of ionic groups in the respective polymers employed. In the study of Chisholm et al.,[51] PBT-ionomers were prepared by the melt polymerization of dimethyl terephthalate, dimethyl 5-sodiosulfoisophthalate, and 1,4-butanediol. Thus the PBT-ionomers had a $-SO_3Na$ group attached onto one of the benzene rings in the sulfonated poly(butylene terephthalate) copolymers. On the other hand, the polymers employed in our study had a $-COONa$ group at the chain end of polystyrene or SI diblock copolymer. Interestingly, Chisholm et al. also noted that the nanocomposite prepared from neat PBT and Clayton HY had very poor dispersion of organoclay aggregates, very similar to our findings from (PSLMW-t-COONa)/MMT nanocomposite (see TEM images given in the Supporting Information).

Using self-consistent mean field theory, Balazs and co-workers[52,53] calculated the free energy profiles as a function of the separation distance between the silicate sheets, as promoted by the penetration of end-functionalized polymer chains. Their theoretical study was based on the premise that attractive interactions between the end-functional group of a polymer chain and the surfactant residing at the surface of an organoclay could be represented by negative values of the Flory–Huggins interaction parameter χ. However, in the present study, we have found that attractive interactions between the $-COO^-$ at the chain end of a PS or SI diblock copolymer and the surfactant (MT2EtOH or 2M2HT) residing at the surface of the organoclay (Cloisite 30B or Cloisite 20A) are realized through ionic association. At present, we have no theoretical guidelines that enable us to determine values of χ for a pair of compounds that have ionic association. Simply put, ionic association (or the formation of ionic clusters) between a pair of compounds cannot be described by the Flory–Huggins interaction parameter χ. Serious effort is needed to develop a theory that will enable one to describe ionic association between a pair of compounds and then to be able to interpret the experimental results presented in this paper.

Acknowledgment. We acknowledge with gratitude that this study was supported in part by the National Science Foundation under Grant CST-04006752 and by LG Chemical Ltd. Southern Clay Products Inc. provided us with the organoclays employed, for which we are very grateful.

Supporting Information Available: GPC traces for (PSLMW-t-COONa)/Cloisite 30B nanocomposite before and

after rheological measurement, XRD patterns and TEM images for (PSLMW-t-COOH)/MMT and (PSLMW-t-COOH)/MMT nanocomposites, and figures summarizing the dynamic frequency sweep data for various nanocomposites based on end-functionalized polystyrene or end-functionalized SI diblock copolymer. This material is available free of charge via the Internet via http://pubs.acs.org.

Note Added after ASAP Publication. This article was released ASAP on September 2, 2005. Equation 1 has been revised. The correct version was posted on September 7, 2005.

References and Notes

(1) (a) Usuki, A.; Kawasumi, M.; Kojima, Y.; Okada, A.; Kurauchi, T.; Kamigaito, O. *J. Mater. Res*. **1993**, *8*, 1174. (b) Kojima, Y.; Usuki, A.; Kawasumi, M.; Okada A.; Kurauchi, T.; Kamigaito, O. *J. Polym. Sci., Polym. Chem. Ed*. **1993**, *31*, 983. (c) Yano, K.; Usuki, A.; Okada, A.; Kurauchi, T.; Kurauchi, T.; Kamigaito, O. *J. Polym. Sci., Polym. Chem. Ed.* **1993**, *31*, 2493.

(2) Messersmith, P. B.; Giannelis, E. P. *Chem. Mater*. **1993**, *5*, 1064.

(3) Messersmith, P. B.; Giannelis, E. P. *J. Polym. Sci., Polym. Phys. Ed*. **1995**, *33*, 1047.

(4) Hoffmann. B.; Kressler, J.; Stöppelmann, G.; Friedrich, C.; Kim, G. M. *Colloid. Polym. Sci.* **2000**, *278*, 629.

(5) Theng, B. K. *The Chemistry of Clay-Organic Reactions*; Wiley: New York, 1974.

(6) Bennett, R. H.; Hulbert, M. H. *Clay Microstructure*; International Human Resources Development Corp.: Boston, 1986.

(7) Over several hundred references are listed under the title of "Clay Nanocomposites" in the Science Finder available on the Internet.

(8) LeBaron, R. C.; Wang, Z.; Pinnavaia, T. *J. Appl. Clay Sci.* **1999**, *15*, 11.

(9) Komori, Y.; Kuroda, K. In *Polymer-Clay Nanocomposites*; Pinnavaia, T. J., Beall, G. W., Eds.; Wiley: New York, 2000; p 3.

(10) Alexandre, M.; Dubois, P. *Mater. Sci. Eng*. **2000**, *28*, 1.

(11) Ray, S. S.; Okamoto, M. *Prog. Polym. Sci*. **2003**, *28*, 1539.

(12) Lee, K. M.; Han, C. D. *Polymer* **2003**, *44*, 4573 and references therein.

(13) Lee, K. M.; Han, C. D. *Macromolecules* **2003**, *36*, 7165 and references therein.

(14) Lee, K. M.; Han, C. D. *Macromolecules* **2003**, *36*, 804.

(15) Choi, S.; Lee, K. M.; Han, C. D. *Macromolecules* **2004**, *37*, 7649.

(16) Wang, Z. M.; Nakajima, H.; Manias, E.; Chung, T. C. *Macromolecules* **2003**, *36*, 8919.

(17) Quirk, R. P.; Yin, J. M. *J. Polym. Sci., Polym. Chem. Ed.* **1992**, *30*, 2349.

(18) Choi, S.; Han, C. D. *Macromolecules* **2003**, *36*, 6220.

(19) Physical Properties Bulletin from Southern Clay Products, Inc.

(20) Grimm, R. E. *Clay Mineralogy*, 2nd ed.; McGraw-Hill: New York, 1968; Chapter 4.

(21) Van Olphen, H. *Clay Colloid Chemistry*, 2nd ed, John Wiley & Sons: New York, 1977; Chapter 5.

(22) Eisenberg, A.; Hird, B.; Moore, R. B. *Macromolecules* **1990**, *23*, 4098.

(23) Hird, B.; Eisenberg, A. *Macromolecules* **1992**, *25*, 6466.

(24) Eisenberg, A.; Smith, P. *Polym. Eng. Sci*. **1982**, *22*, 1117.

(25) Smith, P.; Eisenberg, A. *J. Polym. Sci., Polym. Lett. Ed.* **1983**, *21*, 223.

(26) Rutkowska, M.; Eisenberg, A. *Macromolecules* **1984**, *17*, 821.

(27) Rutkowska, M.; Eisenberg, A. *J. Appl. Polym. Sci.* **1984**, *29*, 755.

(28) Rutkowska, M.; Eisenberg, A. *J. Appl. Polym. Sci.* **1985**, *30*, 3317.

(29) Doi, M.; Edwards, S. F. *The Theory of Polymer Dynamics*; Oxford University Press: Oxford, 1986.

(30) Han, C. D.; Jhon, M. S. *J. Appl. Polym. Sci*. **1986**, *32*, 3809.

(31) Han, C. D.; Kim, J. K. *Macromolecules* **1989**, *22*, 4292.

(32) Han, C. D.; Kim, J. K. *Polymer* **1993**, *34*, 2533.

(33) Han, C. D.; Ma, Y.-J.; Chu, S.-G. *J. Appl. Polym. Sci*. **1986**, *32*, 5597.

(34) Kim, J. K.; Han, C. D.; Lee, Y. J. *Polym. J*. **1992**, *24*, 205.

(35) Yang, H.-H.; Han, C. D.; Kim, J. K. *Polymer* **1994**, *35*, 1503.

(36) Han, C. D.; Kim, J. *J. Polym. Sci., Polym. Phys. Ed.* **1987**, *25*, 1741.

(37) Han, C. D.; Kim, J.; Kim, J. K. *Macromolecules* **1989**, *22*, 383.

(38) Kim, J. K.; Han, C. D. *Macromolecules* **1992**, *25*, 271.

(39) Han, C. D.; Baek, D. M.; Kim, J. K.; Chu, S. G. *Polymer* **1992**, *33*, 294.

(40) Kim, S. S.; Han, C. D. *Macromolecules* **1993**, *26*, 6636.

(41) Kim, S. S.; Han, C. D. *Polymer* **1994**, *35*, 93.

(42) Tachino, H.; Hara, H.; Hirasawa, E.; Kutsumizu, S.; Yano, S. *Macromolecules* **1994**, *27*, 372.

(43) Kutsumizu, S.; Hara, H.; Tachino, H.; Shimabayashi, K.; Yano, S. *Macromolecules* **1999**, *32*, 6340.

(44) There are 5 g of organoclay (Cloisite 30B or Cloisite 20A) in 100 g of nanocomposite. According to the Physical Properties Bulletin from Southern Clay Products (see ref 19), Cloisite 30B contains 90 mequiv of surfactant MT2EtOH, and Cloisite 20A contains 94 mequiv of surfactant 2M2HT. Thus, we estimate the amounts of cation to be $5 \times (90/100) = 4.5$ mequiv in 100 g of (PSLMW-t-COONa)/Cloisite 30B nanocomposite, and $5 \times (94/100) = 4.75$ mequiv in 100 g of (PSLMW-t-COONa)/Cloisite 20A nanocomposite. The amounts of $-COO^-$ ions in 100 g of nanocomposite are calculated as follows. Because each nanocomposite contains 95 wt % end-functionalized polystyrene with the weight-average molecular weight being 2.7×10^4 for PSLMW and 7.0×10^4 for PSHMW, we estimate the amounts of carboxylate ion to be $95/27\,000 = 3.51$ mequiv in the PSLMW-t-COONa nanocomposite, and $95/70\,000 = 1.36$ mequiv in the PSHMW-t-COONa nanocomposite.

(45) Gouinlock, E. V.; Porter, R. S. *Polym. Eng. Sci.* **1977**, *17*, 535.

(46) Sakamoto, N.; Hashimoto, T. *Macromolecules* **1998**, *31*, 3292.

(47) Lee, K. M.; Han, C. D. *Macromolecules* **2002**, *35*, 760.

(48) Choi, S.; Han, C. D. *Macromolecules* **2004**, *37*, 215.

(49) Zhao, H.; Shipp, D. A. *Chem. Mater*. **2003**, *15*, 2693.

(50) Hasegawa, N.; Usuki, A. *Polym. Bull.* **2003**, *51*, 77.

(51) Chisholm, B. J.; Moore, R. B.; Barber, G.; Khouri, F.; Hempstead A.; Larsen, M.; Olson, E.; Kelley, J.; Balch G.; Caraher, J. *Macromolecules* **2002**, *35*, 5508.

(52) Balazs, A. C.; Singh, C.; Zhulina, E. *Macromolecules* **1998**, *31*, 8370.

(53) Zhulina, E.; Singh, C.; Balazs, A. C. *Langmuir* **1999**, *15*, 3955.

MA050803C